🔓 **Open Access**

# Intracavity-Pumped, Mid-Infrared Tandem Optical Parametric Oscillator Based on BaGa$_4$Se$_7$ Crystal

Yixin He
Degang Xu
Jiyong Yao
Yuye Wang
Yangwu Guo
Xianli Zhu
Chao Yan
Longhuang Tang
Jining Li
Kai Zhong
Yicheng Wu
Jianquan Yao
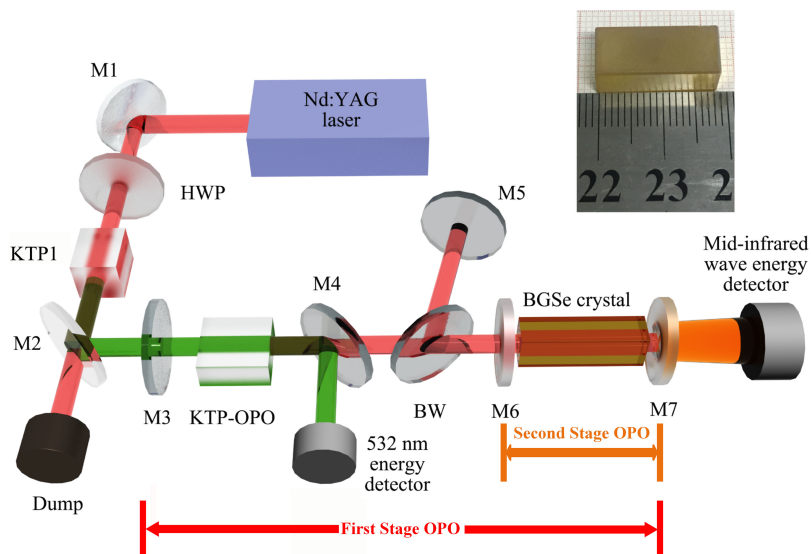
# Intracavity-Pumped, Mid-Infrared Tandem Optical Parametric Oscillator Based on BaGa$_4$Se$_7$ Crystal

**Yixin He** [1,2] **Degang Xu** [1,2] **Jiyong Yao,**[3] **Yuye Wang** [1,2]
**Yangwu Guo,**[3] **Xianli Zhu,**[1,2] **Chao Yan** [1,2] **Longhuang Tang,**[1,2]
**Jining Li** [1,2] **Kai Zhong,**[1,2] **Yicheng Wu,**[4] **and Jianquan Yao**[1,2]

[1]School of Precision Instruments and Optoelectronics Engineering, Institute of Laser and Optoelectronics, Tianjin University, Tianjin 300072, China
[2]Key Laboratory of Optoelectronics Information Technology, Ministry of Education, Tianjin University, Tianjin 300072, China
[3]Beijing Center for Crystal R&D, Key Laboratory of Functional Crystals and Laser Technology, Technical Institute of Physics and Chemistry, Chinese Academy of Sciences, Beijing 100190, China
[4]Institute of Functional Crystal Materials, Tianjin University of Technology, Tianjin 300384, China

**Abstract:** We have demonstrated a tunable mid-infrared tandem optical parametric oscillator (OPO) based on BaGa$_4$Se$_7$ (BGSe) crystal, which was intracavity-pumped by the tunable signal wave at $\sim$1 $\mu$m generated from a KTiOPO$_4$-OPO (KTP-OPO) in doubly-resonant oscillator (DRO) configuration. Wavelength tuning of the mid-infrared tandem OPO was realized by tuning the pump wavelength at the fixed phase matching angle to reduce the effects of beam cutting and Fresnel reflection loss. Together with pump-tuning method, angle-tuning method was supplied to extend tuning range. A tuning range of 4.1–4.5 $\mu$m was obtained with just 5 individual phase matching angles of the BGSe crystal. The maximum output energy of 1.92 mJ/pulse was obtained at 4.26 $\mu$m with an estimated slope efficiency of 9.5%.

**Index Terms:** Nonlinear crystals (BaGa$_4$Se$_7$ crystal), optical parametric oscillator, tunable mid-infrared source.

## 1. Introduction

The tunable mid-infrared wave sources in the wavelength range of 3–5 $\mu$m are especially important for wide applications, such as remote sensing, chemical detection, medicine, and national defense [1], [2]. Tunable mid-infrared lasers above 3 $\mu$m have been realized with mid-infrared quantum cascade laser, interband cascade laser and nonlinear optical (NLO) laser. Mid-infrared quantum cascade lasers and interband cascade lasers based on semiconductors have the advantages of compactness, tunability and room-temperature operation, while relatively complex fabrication process is essential [3], [4]. Optical parametric oscillator (OPO) in NLO laser has the outstanding

characteristics of extremely wide tuning range, narrow linewidth and high output intensity, which are important for valuable applications in spectroscopic science [5]–[7].

NLO crystal is the key element to the performance of the mid-infrared OPO source. Compared with the oxide crystals, the non-oxide crystals have wider transparency spectrum and larger NLO coefficient, which are crucial properties for widely tunable and high-energy mid-infrared OPO source over 4 $\mu$m [8]–[11]. Recently, the newly developed BGSe crystal with high performances is considered as a very promising NLO crystal for widely tunable and high-energy mid-infrared wave generation, especially pumped at 1 $\mu$m [12]–[16]. BGSe crystals with long length (14.5–30 mm) have been employed in the widely tunable and high-energy mid-infrared OPO sources, which were pumped by different fixed wavelengths of 1.053 $\mu$m, 1.064 $\mu$m, 2.1 $\mu$m and 2.79 $\mu$m under type I and type II phase-matching (PM) conditions [17]–[22] with angle-tuning method. Except for the angle-tuning method, many tuning methods have been employed in the OPO sources instead of tilting the angle of crystals, including temperature-tuning and pump-tuning methods. Pump-tuning method is an efficient method to realize tunable mid-infrared source, with the advantages of wide tuning range, stable output energy and easy tuning [23].

Tandem OPO, as a kind of structure for pump-tuning method, have been adopted in uncritical configuration with periodically poled crystal [24]–[27], AgGaSe$_2$ [28], [29] and ZnGaP$_2$ [23], [30]–[34]. It is promising to generate wavelength-agile and continuously scanning mid-infrared wave without tilting the crystal. In the aspect of pumping method, the BGSe-OPO was external-cavity pumped. Intracavity pump condition with the advantages of higher pump density and compact design has not been applied in BGSe-OPOs [35].

In this paper, an intracavity-pumped mid-infrared tandem OPO based on BGSe crystal was demonstrated. The BGSe-OPO was pumped by a wavelength tunable KTP-OPO ($\sim$1052–1063 nm) in DRO configuration to improve the pump energy intensity. Compared with the tuning range of $\sim$15 nm in the BGSe-OPO with angle-tuning method, the tuning range was experimentally extended to $\sim$100 nm without rotating the BGSe crystal in tandem OPO. Together with angle-tuning method, a tuning range of 4.1–4.5 $\mu$m was obtained in tandem BGSe-OPO. Further extension of the tuning range would be easily achieved by adopting a much wider tuning pump. The maximum output energy of 1.92 mJ/pulse was obtained at 4.26 $\mu$m with an estimated slope efficiency of 9.5%. The characteristics of the output energy, wavelength tuning, temporal width and the beam divergence of the generated mid-infrared wave were also investigated.

## 2. Experimental Details

The schematic diagram of the mid-infrared tandem OPO is shown in Fig. 1. The fundamental pump wave with a beam diameter of 4 mm was generated by a high-energy Nd:YAG laser (Spectra-Physics, 1064 nm, 200 mJ, 14 ns, 10 Hz) with a linewidth of $\sim$30 GHz. The 1064 nm pump wave was reflected into KTP1 crystal (7 $\times$ 7 $\times$ 10 mm$^3$, $\theta = 90°$, $\varphi = 23.5°$) for second harmonic generation (SHG) by M1. A half-wave plate (HWP) was used to control the phase-matching condition of SHG. The energy controllable 532 nm green light was reflected by the mirror M2, which was highly reflective (HR) at 532 nm and highly transmissive (HT) coated at 1064 nm with 45° incident, to pump the KTP-OPO. The fundamental single-pass KTP-OPO in the first stage consisted of plane parallel mirrors M3 (532 nm HT, 1 $\mu$m HR), M5 (532 nm HT, 1 $\mu$m HR), M7 (1 $\mu$m & 1.3–1.6 $\mu$m HR, 3–5 $\mu$m HT) and KTP crystal (8 $\times$ 10 $\times$ 20 mm$^3$, $\theta = 90°$, $\varphi = 25°$). The depleted 532 nm green light was filtered out by M4 (532 nm HR incident at 45°, 1 $\mu$m HT incident at 45°) to avoid possible damage to the BGSe crystal. The energy of the depleted 532 nm green light ($E_{1@532nm}$) was measured by the energy detector (Newport Corporation, 919E-10-20-250) to estimate the energy of tunable signal $\lambda$1 ($E_{\lambda 1}$). Besides the nonlinear process of OPO, we assumed that there was no extra loss of the 532 nm green light. Thus, all the depletion photons of the 532 nm green light were transferred to the equal number of signal and idler photons. Due to the near degenerate point KTP crystal, the photon energies of signal and idler waves were almost the same. Therefore, the energy of $\lambda$1 was approximately estimated to be proportional to the half of the depletion of the energy of 532 nm green light ($E_{de@532nm}$) as $E_{\lambda 1} \propto E_{de@532nm}/2 = (E_{input@532nm} - E_{1@532nm})/2$.
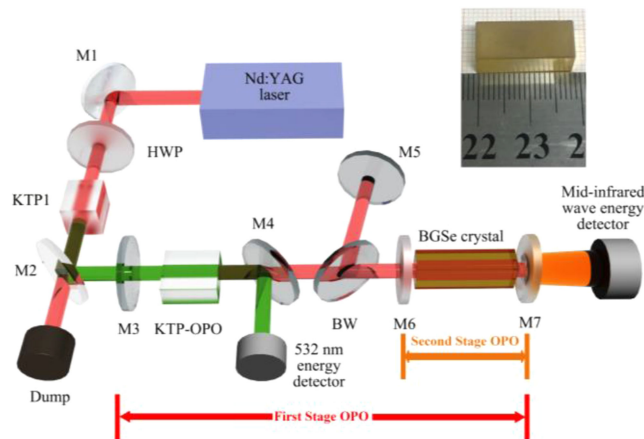
Fig. 1. Schematic diagram of mid-infrared tandem OPO based on BGSe crystal (inset shows the BGSe crystal).

A Brewster window (BW) in the fundamental doubly-resonant KTP-OPO cavity was employed to realize a dual-cavity configuration (M3–M7 & M3–M5) with the same cavity length of 250 mm, in which the orthogonal polarizations of signal ($\lambda 1$) and idler ($\lambda 2$) waves were resonating separately. The generated tunable $\lambda 1$ with horizontal polarization was adopted to pump the mid-infrared OPO source based on BGSe crystal in the second stage. Calcium fluoride mirrors M6 (1 $\mu$m HT, 1.3–1.6 $\mu$m & 3–5 $\mu$m HR) and M7 composed the intracavity BGSe-OPO, with a cavity length of 40 mm. The BGSe crystal with the dimension of 8 $\times$ 8 $\times$ 18.8 mm$^3$ (length) was cut at $\theta = 53.4°$ based on the Sellmeier equation for type-I PM condition (o-ee), and was HT coated at 1 $\mu$m & 3–5 $\mu$m & 1.3–1.6 $\mu$m to reduce the cavity loss. The generated tunable mid-infrared wave was measured by the mid-infrared energy detector (Newport Corporation, 919E-0.1-12-25K). A calcium fluoride dichroic mirror (1 $\mu$m & 1.3–1.6 $\mu$m HR, 3–5 $\mu$m HT) was placed before the window of the detector to avoid the influence of the near-infrared waves. Wavelengths of the generated mid-infrared waves ($\lambda 3$) were calculated by the wavelength differences between the $\lambda 1$ and the signal waves of BGSe-OPO, measured by the spectrometer (Yokogawa, AQ6370) at the resolution of 0.05 nm.

## 3. Results and Discussion

The tunable $\lambda 1$ generated by near degenerate point KTP-OPO in the first stage was adopted to pump the BGSe-OPO in the second stage. The energy intensity of $\lambda 1$ can be enhanced with the employment of M5, which was used to achieve a feedback for $\lambda 2$. To confirm the significant pumping improvement of KTP-OPO with M5, the output energies of the tandem OPO were compared with and without M5, when the BGSe crystal was set to be incident normally in the cavity and $\lambda 1$ was 1062.3 nm. Fig. 2(a) shows the input-output characteristics of the tandem OPO with and without M5 at 4.26 $\mu$m. The relationship between the energies of the generated mid-infrared waves and the depletion of the 532 nm green light is shown as Fig. 2(b). It can be observed that the threshold of the tandem OPO with M5 was about 60 mJ/pulse, slightly lower than that without M5 ($\sim$65 mJ/pulse). The threshold difference between DRO (with M5) and singly-resonant oscillator (SRO, without M5) should be much larger than the experimental results based on OPO theory [30]. It was due to that the KTP-OPO in the first stage was actually degraded into an intermediate SRO-DRO by the equivalent nonlinear loss of $\lambda 1$, acting as the pump for the BGSe-OPO in the second stage [30], [35]. When the tandem OPO system was pumped at input 532 nm energy of 135 mJ/pulse, the maximum output energy of 1.92 mJ/pulse at 4.26 $\mu$m was obtained in the tandem OPO with M5. Meanwhile, the maximum output energy of 1.18 mJ/pulse was obtained without M5 at the same pump energy. Furthermore, the mid-infrared wave output with M5 was
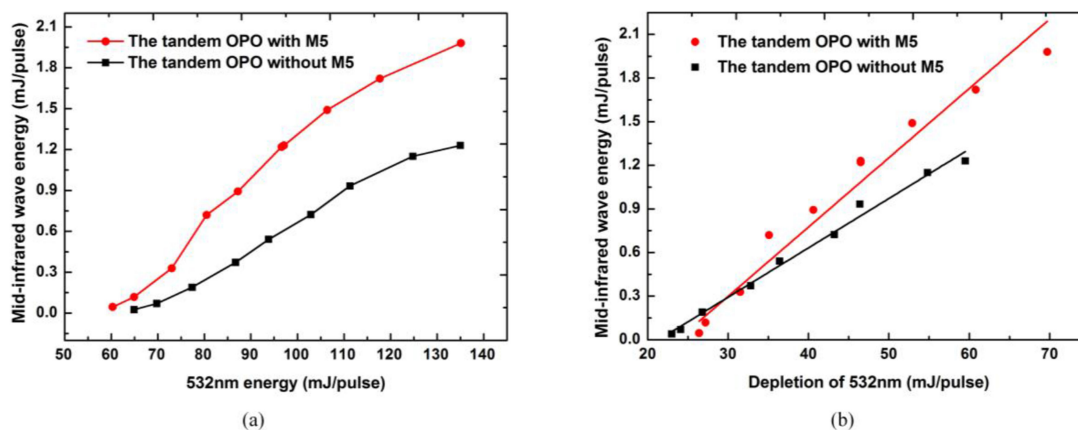
Fig. 2. (a) Input-output characteristics of tandem OPO with and without M5. (b) The relationship between the energies of the generated mid-infrared wave at 4.26 $\mu$m and the depletion of the 532 nm green light.
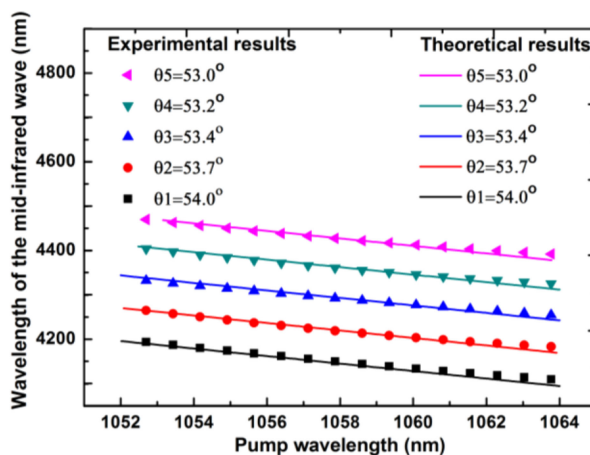


Fig. 3. Output wavelength of mid-infrared tandem OPO pumped by tunable $\lambda$1.

much higher than that without M5 in the whole tuning range. Based on the energy estimation of $\lambda$1, the overall slope efficiency of the tandem OPO with M5 was estimated to be ~9.5%, much higher than ~6.8% without M5. And the photon conversion efficiency from $\lambda$1 to $\lambda$3 was estimated to be 22.1% with M5 much higher than 16.8% without M5. Overall, due to the much higher energy intensity of the tunable $\lambda$1 oscillated in the cavity, the tandem OPO with M5 was obviously optimum for the generation of mid-infrared wave. Compared with the recent experimental results of ZGP-OPO and BGSe-OPO [34], [21], the conversion efficiency and slope efficiency were limited by the ~1 $\mu$m pump in our experiment. This was attributed to the large quantum defect under short pump wavelength. Considering the ~1 $\mu$m pump source was much more economic and convenient, the tandem BGSe-OPO in our experiment provided an efficient way to generate tunable mid-infrared wave.

Without rotating the BGSe crystal, the tuning characteristics of the tandem mid-infrared source in the optimized DRO configuration can be effectively realized by employing a tunable pump wave. This method can effectively reduce the beam cutting effect and reflection loss mentioned above. When the pump wavelength was tuned in the range of 1052–1063 nm, a tuning range of 4.1–4.5 $\mu$m in the mid-infrared tandem OPO was obtained at five individual PM angles of $\theta$1−$\theta$5 (54.0°, 53.7°, 53.4°, 53.2° and 53.0°), shown as dots in Fig. 3. Additionally, the tuning range of mid-infrared
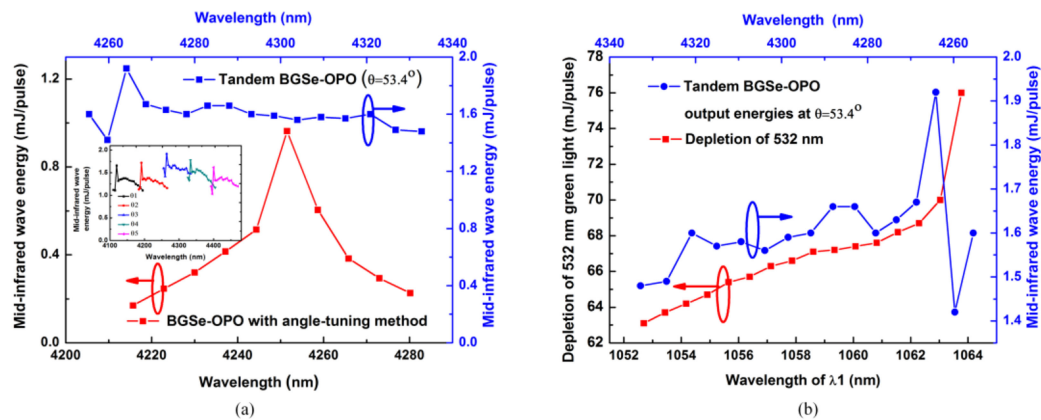
Fig. 4. (a) Tuning characteristics of the generated mid–infrared waves of the tandem OPO at $\theta 3$ and BGSe-OPO with angle-tuning method (inset shows the tuning characteristics of tandem BGSe-OPO at $\theta 1-\theta 5$ with pump-tuning method). (b) The depletion of 532 nm green light at different wavelengths of $\lambda 1$ and the output energies of the tandem BGSe-OPO pumped by tunable $\lambda 1$.

tandem OPO was theoretically calculated by Sellmeier equation in [36], shown as lines in Fig. 3, fitting well with the experimental results. Further extension of the tuning ability can be realized by employing KTP-OPO with wider tuning range.

Beam cutting and Fresnel reflection loss limit the output energy and tuning range of BGSe-OPO with angle-tuning method [18], especially for the crystal with small cross section and large length. Here, a mid-infrared OPO based on a similar BGSe crystal ($4 \times 4 \times 18.8$ mm$^3$, $\theta = 53.4°$) pumped with Nd:YAG laser at 16 mJ/pulse was demonstrated as a comparison for our tandem OPO. Fig. 4(a) shows the tuning characteristics of BGSe-OPO with angle-tuning method and tandem BGSe-OPO with pump-tuning method. The maximum output energy of the BGSe-OPO with angle-tuning method was $\sim$1 mJ/pulse at 4.25 $\mu$m. It should be mentioned that the BGSe crystal just can be rotated in a very small range to realize the wavelength tuning due to beam cutting effect. The FWHM of tuning range was measured to be $\sim$15 nm. In comparison with the angle-tuning method, although no rotation of the BGSe crystal was adopted in the tandem BGSe-OPO, the tuning range was extended to $\sim$90 nm with a relatively flat output energy over 1.4 mJ/pulse.

To obtain a much wider tuning range of the mid-infrared tandem OPO, two tuning methods of changing the PM angles of the BGSe crystal and tuning the pump wavelengths were both adopted. With this integrated tuning method, a wide tuning range of 4.1–4.5 $\mu$m was obtained in the mid-infrared tandem OPO based on BGSe crystal under the pump energy of 135 mJ/pulse at 532 nm. And in the entire tuning range, only output energies of $>$1 mJ was recorded to guarantee the practicality. The inset in Fig. 4(a) shows the tuning characteristics of the mid-infrared tandem OPO. Pumped by the tunable $\lambda 1$ (1052–1063 nm) generated by the KTP-OPO, the obtained tuning ranges of the mid-infrared waves were 4.11–4.19 $\mu$m, 4.18–4.27 $\mu$m, 4.25–4.33 $\mu$m, 4.32–4.40 $\mu$m and 4.39–4.47 $\mu$m for the PM angles of $\theta 1-\theta 5$, respectively. The maximum output energies for $\theta 1-\theta 5$ were 1.66 mJ/pulse at 4.12 $\mu$m, 1.72 mJ/pulse at 4.19 $\mu$m, 1.92 mJ/pulse at 4.26 $\mu$m, 1.78 mJ/pulse at 4.33 $\mu$m and 1.62 mJ/pulse at 4.40 $\mu$m, respectively.

On one hand, as for the generated tunable mid-infrared waves at different PM angles, the enhancement of the output energies was observed at normal incidence for $\theta 3$ under the same pumping condition. The cavity loss caused in the second stage OPO by the Fresnel reflection was proportional to the discrepancy to $\theta 3$ while rotating the BGSe crystal. Thus, the output energies of tunable mid-infrared waves at $\theta 2$ and $\theta 4$ were relatively higher than those at $\theta 1$ and $\theta 5$, respectively. On the other hand, as for the generated tunable mid-infrared waves at every fixed PM angle, the output energies of the tandem OPO was enhanced when $\lambda 1$ was 1062.3 nm. With $\lambda 1$ shorter than 1062.3 nm, the output energies of the tandem OPO decreased gradually. The energy intensities
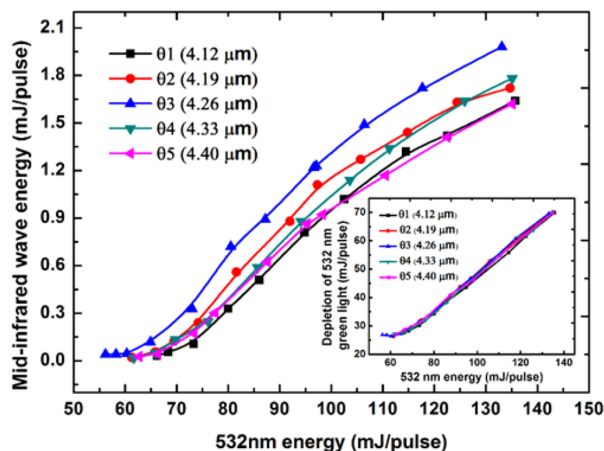
Fig. 5. The input-output characteristics of the generated mid-infrared waves (inset shows the depletion of 532 nm green light at different PM angles).

of $\lambda 1$ at different wavelengths were qualitatively characterized by measuring the depletion of the 532 nm green light, as shown in Fig. 4(b). It can be seen that the energy intensity of $\lambda 1$ dropped at shorter wavelength, due to the extra reflection loss while rotating the KTP crystal. This trend was in accordance with the attenuation of the mid-infrared wave output energies at shorter pump wavelength of $\lambda 1$ in Fig. 4(b). Thus, it was deduced that, the observed attenuation phenomenon of the tandem OPO under $\lambda 1$ shorter than 1062.3 nm was related to the energy intensity reduction of $\lambda 1$ in the cavity. Furthermore, the energy intensity of $\lambda 1$ increased remarkably as approaching the degenerate point of the KTP crystal. However, the mid-infrared output energies were dramatically decreased when the pump wavelength was longer than 1062.3 nm at every fixed PM angle, which didn't agree with the expectation. This means that, besides the energy intensity of $\lambda 1$, the mid-infrared output energy would be affected by other factors, including the linewidth broadening effect of $\lambda 1$ [37], which was observed to be broadened from 0.15 nm to 1 nm in experiment as approaching the degenerate point of the KTP crystal. Although the tuning range of the current experimental setup was not wide enough due to the $\sim$10 nm tuning range of $\lambda 1$, the tandem OPO is still a much efficient approach to eliminate the non-intrinsic loss in the BGSe-OPO if the OPO in the first stage could be optimized to obtain a wide tuning range and flat output.

Fig. 5 shows the output mid-infrared wave energies versus the pump energy of 532 nm green light at 4.12 $\mu$m ($\theta 1$), 4.19 $\mu$m ($\theta 2$), 4.26 $\mu$m ($\theta 3$), 4.33 $\mu$m ($\theta 4$) and 4.40 $\mu$m ($\theta 5$), when $\lambda 1$ was set to be 1062.3 nm. The input-output characteristics of $\lambda 1$ were indicated by the depletion of the 532 nm, as shown in the inset of Fig. 5. The thresholds of the mid-infrared tandem OPO at different PM angles were different, due to the different cavity losses of the BGSe-OPO. A saturation phenomenon of the generated mid-infrared waves was observed in the output of the tandem OPO. However, the energy intensities of $\lambda 1$ were estimated to be increasing monotonically and linearly without saturation. And the energy intensities of $\lambda 1$ were almost the same at different PM angles of $\theta 1$–$\theta 5$. It means that due to the relatively low conversion efficiency, $\lambda 1$ generated by KTP-OPO in the first stage was not sensitive to the BGSe-OPO in the second stage. The KTP-OPO and the BGSe-OPO processes were observed to be relatively independent. Moreover, the saturation phenomenon of the BGSe-OPO appeared before KTP-OPO, which was related to the different cavity lengths of BGSe-OPO and KTP-OPO.

Fig. 6 shows the temporal pulse profiles (arbitrarily normalized to a common maximum) of depleted $\lambda 1$ (1062.3 nm), undepleted $\lambda 1$ and the generated mid-infrared wave at 4.26 $\mu$m, measured by InGaAs photodiode (Thorlabs, DET08C) and (HgCdZn) Te photodiode (Vigo, PCI-9), respectively. The temporal pulse profiles of depleted and undepleted $\lambda 1$ were recorded with and without the BGSe crystal in the cavity. The pulse widths of the depleted and the undepleted $\lambda 1$ were 6.73 ns
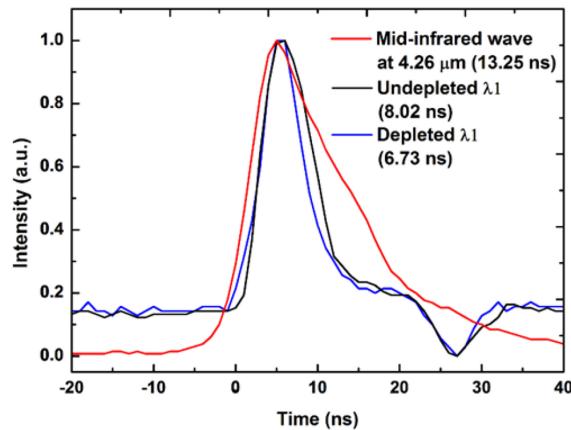
Fig. 6. The temporal profile of the depleted λ1, undepleted λ1, and the mid-infrared wave.
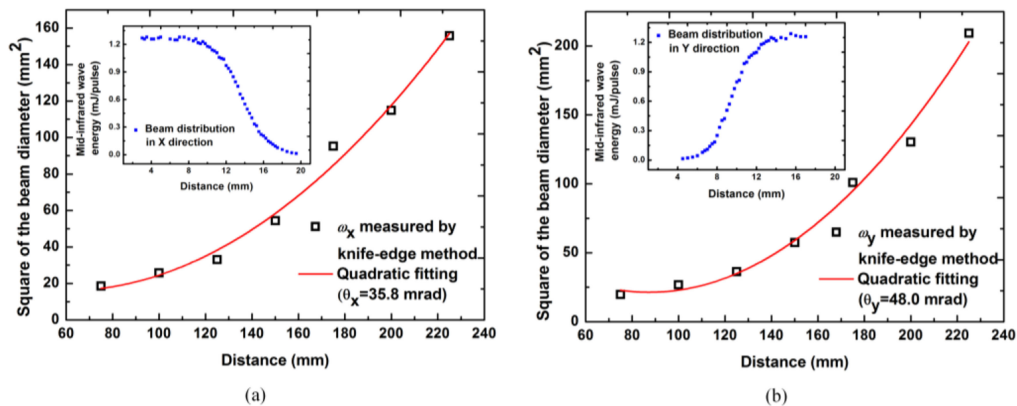


Fig. 7. (a) Diameters of generated mid-infrared beam in X direction (inset shows the beam distribution in X direction). (b) Diameters of generated mid-infrared beam in Y direction (inset shows the beam distribution in Y direction).

and 8.02 ns, respectively. It was clearly observed that the pulse of λ1 was depleted when the BGSe-OPO was operating. The pulse width of the mid-infrared wave at 4.26 $\mu$m was 13.25 ns, which was measured to be wider than λ1 due to the different rise times of the detectors.

The beam sizes of the generated mid-infrared wave at 4.26 $\mu$m were measured by the knife-edge method at different distances from output window (M7) in the horizontal (X) and vertical (Y) directions, as shown in Fig. 7(a)–(b). The insets show the spatial distributions of the beam cross sections at the distance of 100 mm. The beam of the generated mid-infrared wave had a good shape of Gaussian distribution in X and Y directions. By quadratic fitting method, the divergence angles of the generated mid-infrared wave were calculated to be 35.8 mrad and 48 mrad in X and Y directions. Compared with the approximate circular beam shape in the near field, the beam shape was elliptical in the far field. The beam deterioration was limited by multiple OPO processes. Further improvement to the beam quality and the conversion efficiency would be performed by adopting non-critical phase matching (NCPM) condition in the first stage, MOPA pumping configuration and optimal cavity design in the mid-infrared tandem OPO [38].

## 4. Conclusion

A mid-infrared tandem OPO based on BGSe crystal was demonstrated. The BGSe crystal was intracavity-pumped by a tunable KTP-OPO in DRO configuration. Pump-tuning method was adopted

to the mid-infrared tandem OPO to reduce the beam cutting effect and reflection loss, etc. Supplied with angle-tuning method, the tuning range of the tandem mid-infrared source of 4.1–4.5 $\mu$m was obtained. The maximum output energy of 1.92 mJ/pulse was obtained at 4.26 $\mu$m. The tuning range, output energy and the beam divergence of the mid-infrared tandem OPO can be further improved by employing NCPM, MOPA and optimizing the cavity structure.

## References

[1] U. Simon, Z. Benko, M. W. Sigrist, R. F. Curl, and F. K. Tittel, "Design considerations of an infrared spectrometer based on difference-frequency generation in AgGaSe$_2$," *Appl. Opt.*, vol. 32, no. 33, pp. 6650–6655, Nov. 1993.

[2] T. H. Allik, S. Chandra, D. M. Rines, P. G. Schunemann, J. Andrew Hutchinson, and R. Utano, "Tunable 7–12-$\mu$m optical parametric oscillator using a Cr,Er:YSGG laser to pump CdSe and ZnGeP$_2$ crystals," *Opt. Lett.*, vol. 22, no. 9 pp. 597–599, May 1997.

[3] M. S. Vitiello, G. Scalari, B. Williams, and P. De Natale, "Quantum cascade lasers: 20 years of challenges," *Opt. Exp.*, vol. 23, no. 4, pp. 5167–5182, Feb. 2015.

[4] R. Q. Yang *et al.*, "InAs-band interband cascade lasers," *IEEE J. Sel. Top. Quantum Electron.*, vol. 25, no. 6, Nov. 2019, Art. no. 1200108.

[5] L. J. Lin and J. L. Montgomery, "Generation of tunable mid-ir (1.8–2.4 $\mu$m) laser from optical parametric oscillation in KTP," *Opt. Commun.*, vol. 75, no. 3, pp. 315–320, Aug. 1990.

[6] Y. X. Fan, R. C. Eckardt, R. L. Byer, R. K. Route, R. S. Feigelson, "AgGaS$_2$ infrared parametric oscillator," *Appl. Phys. Lett.*, vol. 45, no. 4, pp. 313–315, May 1984.

[7] X. Duan, L. Li, Y. Shen, B. Yao, and Y. Wang, "Efficient middle-infrared ZGP-OPO pumped by a Q-switched Ho: LuAG laser with the orthogonally polarized pump recycling scheme," *Appl. Opt.*, vol. 57, no. 27, pp. 8102–8107, Aug. 2018.

[8] X. Zhang, J. Yao, W. Yin, Y. Zhu, Y. Wu, and C. Chen, "Determination of the nonlinear optical coefficients of the BaGa$_4$Se$_7$ crystal," *Opt. Exp.*, vol. 23, no. 1, pp. 552–558, Jan. 2015.

[9] V. Petrov, "Parametric down-conversion devices: The coverage of the mid-infrared spectral range by solid-state laser sources," *Opt. Mater.*, vol. 34, no. 3, pp. 536–554, Mar. 2011.

[10] V. Petrov, "Progress in 1-$\mu$m pumped mid-IR optical parametric oscillators based on non-oxide nonlinear crystals," *IEEE J. Sel. Top. Quantum Electron.*, vol. 21, no. 1, Jan. 2015, Art. no. 1602914.

[11] V. Petrov, "Frequency down-conversion of solid-state laser sources to the mid-infrared spectral range using non-oxide nonlinear crystals," *Prog. Quant. Electron.*, vol, 42, pp. 1–106, Jul. 2015.

[12] J. Yao, D. Mei, L. Bai, Z. Lin, W. Yin, P. Fu, and Y. Wu, "BaGa$_4$Se$_7$: A new congruent-melting IR nonlinear optical material," *Inorg. Chem.*, vol. 49, no. 20, pp. 9212–9216, Sep. 2010.

[13] Y. He *et al.*, "High energy and tunable mid-infrared source based on BaGa$_4$Se$_7$ crystal by single-pass difference-frequency generation," *Opt. Exp.*, vol. 27, no. 6, pp. 9241–9249, Mar. 2019.

[14] J. Yao *et al.*, "Growth and characterization of BaGa$_4$Se$_7$ crystal," *J. Cryst. Growth*, vol. 346, no. 1, pp. 1–4, Mar. 2012.

[15] A. A. Boyko *et al.*, "Intracavity difference-frequency mixing of optical parametric oscillator signal and idler pulses in BaGa$_4$Se$_7$," *Appl. Opt.*, vol. 56, no. 10, pp. 2783–2786, Apr. 2017.

[16] E. Boursier *et al.*, "Phase-matching directions and refined Sellmeier equations of the monoclinic acentric crystal BaGa$_4$Se$_7$," *Opt. Lett.*, vol. 41, no. 12, pp. 2731–2734, Jun. 2016.

[17] N. Y. Kostyukova *et al.*, "Widely tunable in the mid-IR BaGa$_4$Se$_7$ optical parametric oscillator pumped at 1064 nm," *Opt. Lett.*, vol. 41, no. 15, pp. 3667–3670, Aug. 2016.

[18] W. Xu *et al.*, "High-pulse-energy mid-infrared optical parametric oscillator based on BaGa$_4$Se$_7$ crystal pumped at 1.064 $\mu$m," *Appl. Phys. B*, vol. 123, no. 80, pp. 1–6, Mar. 2017.

[19] J. Yuan *et al.*, "High power, tunable mid-infrared BaGa$_4$Se$_7$ optical parametric oscillator pumped by a 2.1 $\mu$m Ho: YAG laser," *Opt. Exp.*, vol. 24, no. 6, pp. 6083–6087, Mar. 2016.

[20] B. Zhao *et al.*,"High-efficiency, tunable 8–9 $\mu$m BaGa$_4$Se$_7$ optical parametric oscillator pumped at 2.1 $\mu$m," *Opt. Mater. Exp.*, vol. 8, no. 11, pp. 3332–3337. Oct. 2018.

[21] S. Hu *et al.*, "High-conversion-efficiency tunable mid-infrared BaGa$_4$Se$_7$ optical parametric oscillator pumped by a 2.79-$\mu$m laser," *Opt. Lett.*, vol. 44, no. 9, pp. 2201–2203, May 2019.

[22] D. B. Kolker *et al.*, "Widely tunable (2.6–10.4 $\mu$m) BaGa$_4$Se$_7$ optical parametric oscillator pumped by a Q-switched Nd: YLiF$_4$ laser," *J. Phys. Commun.*, vol. 2, no. 3, Mar. 2018, Art. no. 035039.

[23] K. Miyamoto and H. Ito, "Wavelength-agile mid-infrared (5–10 $\mu$m) generation using a galvano-controlled KTiOPO$_4$ optical parametric oscillator," *Opt. Lett.*, vol. 32, no. 3, pp. 274–276, Feb. 2007.

[24] K. L. Vodopyanov *et al.*, "Optical parametric oscillation in quasi-phase-matched GaAs," *Opt. Lett.*, vol. 29, no. 16, pp. 1912–1914, Aug. 2004.

[25] P. S. Kuo *et al.*, "Optical parametric generation of a mid-infrared continuum in orientation-patterned GaAs," *Opt. Lett.*, vol. 31, no. 1, pp. 71–73, Jan. 2006.

[26] P. V. Gorelik, F. N. Wong, D. Kolker, and J. Zondy, "Cascaded optical parametric oscillation with a dual-grating periodically poled lithium niobate crystal," *Opt. Lett.*, vol. 31, no. 13, pp. 2039–2041, Jul. 2006.

[27] K. L. Vodopyanov, I. Makasyuk, and P. G. Schunemann, "Grating tunable 4–14 $\mu$m GaAs optical parametric oscillator pumped at 3 $\mu$m," *Opt. Exp.*, vol. 22, no. 4, pp. 4131–4136, Feb. 2014.

[28] H. Komine, J. M. Fukumoto, W. H. Long, and E. A. Stappaerts, "Noncritically phase matched mid-infrared generation in AgGaSe$_2$," *IEEE J. Sel. Top. Quantum Electron.*, vol. 1, no. 1, pp. 44–49, Apr. 1995.

[29] S. Chandra, T. H. Allik, G. Catella, R. Utano, and J. A. Hutchinson, "Continuously tunable, 6–14 $\mu$m silver-gallium selenide optical parametric oscillator pumped at 1.57 $\mu$m," *Appl. Phys. Lett.*, vol. 71, no. 5, pp. 584–586, Aug. 1997.

[30] P. B. Phua, K. S. Lai, R. F. Wu, and T. C. Chong, "Coupled tandem optical parametric oscillator (OPO): An OPO within an OPO," *Opt. Lett.,* vol. 23, no. 16, pp. 1262–1264, Aug. 1998.

[31] P. B. Phua, K. S. Lai, R. F. Wu, and T. C. Chong, "High-efficiency mid-infrared ZnGeP$_2$ optical parametric oscillator in a multimode-pumped tandem optical parametric oscillator," *Appl. Opt.,* vol. 38, no. 3, pp. 563–565, Jan.1999.

[32] K. L. Vodopyanov and P. G. Schunemann, "Broadly tunable noncritically phase-matched ZnGeP$_2$ optical parametric oscillator with a 2-$\mu$J pump threshold," *Opt. Lett.,* vol. 28, no. 6, pp. 441–443, Mar. 2003.

[33] S. Das, "Pump tuned wide tunable noncritically phase-matched ZnGeP$_2$ narrow line width optical parametric oscillator," *Infrared Phys. Tech.,* vol. 69, pp. 13–18, Mar. 2015.

[34] B. Cole *et al.,* "Compact and efficient mid-IR OPO source pumped by a passively Q-switched Tm: YAP laser," *Opt. Lett.,* vol. 43, no. 5, pp. 1099–1102, Mar. 2018.

[35] A. A. Boyko *et al.,* "Intracavity-pumped, cascaded AgGaSe$_2$ optical parametric oscillator tunable from 5.8 to 18 $\mu$m," *Opt. Exp.,* vol. 23, no. 26, pp. 33460–33465, Dec. 2015.

[36] F. Yang *et al.,* "Midinfrared optical parametric amplifier with 6.4–11, range based on BaGa$_4$Se$_7$," *IEEE Photon. Technol. Lett.,* vol. 27, no. 10, pp. 1100–1103, May 2015.

[37] K. L. Vodopyanov and V. G. Voevodin, "Type I and II ZnGeP$_2$ travelling-wave optical parametric generator tunable between 3.9 and 10 $\mu$m," *Opt. Commun.,* vol. 117, pp. 277–282, Jun. 1995.

[38] G. Stoeppler, N. Thilmann, V. Pasiskevicius, A. Zukauskas, C. Canalias, and M. Eichhorn, "Tunable mid-infrared ZnGeP$_2$ RISTRA OPO pumped by periodically-poled Rb:KTP optical parametric master-oscillator power amplifier," *Opt. Exp.,* vol. 20, no. 4, pp. 4509–4517, Feb. 2012.